Polyhedron 52 (2013) 733–742

Contents lists available at SciVerse ScienceDirect

Polyhedron

journal homepage: www.elsevier.com/locate/poly

Spectroscopic and structural insights into *N*-substituted pyridinium-4-aldoximes and their pentacyanoferrate(II) complexes

Blaženka Foretić [a,*], Igor Picek [a,*], Vladimir Damjanović [a], Danijela Cvijanović [a], Ivana Pulić [b], Boris-Marko Kukovec [b], Dubravka Matković-Čalogović [b]

[a] Department of Chemistry and Biochemistry, Faculty of Medicine, University of Zagreb, Šalata 3, 10000 Zagreb, Croatia
[b] Department of Chemistry, Faculty of Science, University of Zagreb, Horvatovac 102a, 10000 Zagreb, Croatia

ARTICLE INFO

Article history:
Available online 3 August 2012

Dedicated to Alfred Werner on the 100th Anniversary of his Nobel Prize in Chemistry in 1913.

Keywords:
Pyridinium-4-aldoxime derivatives
Pentacyanoferrates(II)
Aqueous equilibria
Kinetics
Spectroscopy

ABSTRACT

Comparative kinetic and equilibrium studies on the formation and dissociation of three mono- and one bis-pyridinium-4-aldoxime pentacyanoferrate(II) complexes have been carried out in aqueous solutions at 25 °C and $I = 0.1$ M. The synthesis, spectroscopic and thermal characterization of a new *N*-methylpyridinium-4-aldoxime pentacyanoferrate(II) complex is presented. The obtained values for the equilibrium constants, identified as apparent formation constants (β_f/M^{-1}) along with kinetic parameters, the formation ($k_f/M^{-1}\,s^{-1}$) and dissociation (k_d/s^{-1}) rate constants indicated the behaving of all protonated pyridinium-4-aldoximes as weak π-acceptors. The pH-dependence of the dissociation rates has been analyzed in terms of ionization abilities of the coordinated ligands. The magnitude of the dissociation rates suggested that both protonated and deprotonated ligand forms are effective σ-donors that bind to the $[Fe(CN)_5]^{3-}$ moiety through the nitrogen atom. The deprotonation of the coordinated aldoxime group leads to the reduced lability of the complexes due to increased σ-donor capability of aldoximato nitrogen causing the strengthened of the iron(II)–nitrogen bond. The values of dissociation activation parameters, $\Delta H^{\ddagger}$ and $\Delta S^{\ddagger}$, are found to be consistent with the S_N1 dissociative type of mechanism. The spectroscopic data (FT-IR, NMR and UV–Vis) of the isolated coordinated pentacyanoferrates(II) conforms with the weak π-acceptor properties of the pyridinium-4-aldoxime ligands. A detailed structural characterization of the iodide and chloride salt of *N*-methylpyridinium-4-aldoxime was also presented using NMR, FT-IR and UV–Vis spectroscopy, as well as X-ray diffraction.

© 2012 Elsevier Ltd. All rights reserved.

1. Introduction

The mono- and bis-pyridinium oximes as quaternized derivatives of pyridyl oximes are known as pharmacologically important agents. Explicitly the ionization of oxime group produces powerful nucleophilic oximato form, widely used in the hydrolytic cleavage of either phosphoric and carboxylic acid esters or amides [1]. The positive charge present in the pyridinium moiety is responsible for the fact that pK_a of oxime group is 3–5 pK_a units lower when compared to a parent pyridyl oxime ($10 \leqslant pK_a \leqslant 12$). Besides, the coordination of pyridyl oximes to metal increases the acidity in the coordinated ligands making them important as hydrolytic catalysts in physiological conditions [2]. Investigations of the acidity–nucleophilicity relationship revealed that the reactivity of complexed pyridyl oximates depends not only on the nature of the bound metal ion, but also on the structure of the oxime ligand. Unlike the pyridinium oximes, the coordination chemistry of pyridyl oximes has been well documented [3], describing the immense structural diversity and properties of the complexes with monoanions of simple pyridyl oximes that exhibit many distinct coordination modes. Currently, only formation of the pyridinium oxime complex with palladium(II) [4a] and, of particular relevance to our investigations, the complexes with the pentacyanoferrate(II) moiety were reported [4b–h], but only limited characterization data were presented at the time. A more detailed studies of the structure and reactivity toward the aquapentacyanoferrate(II), $[Fe(CN)_5(H_2O)]^{3-}$, of some *N*-phenacyl- and *N*-benzoylethylpyridinium-4-aldoximes were recently reported [5]. Acidic properties and nucleophilicity of the mono- and bis-pyridinium aldoximes make them well known as effective antidotes against poisoning by organophosphates which cause long-term inactivation of acetylcholinesterase (AChE, E.C.3.1.1.7) [6]. The positive charge in the pyridinium moiety site-directs reactivation of the enzyme catalytic site providing the cleavage of a serine-bounded phosphate by the aldoximato moiety. Many of pyridinium aldoximes have also shown other significant and versatile bioactivities [7] which are evidently closely related to the interplay of their structure, acidic properties and coordination ability. Therefore, their reactivity

* Corresponding authors. Tel.: +385 1 4566 760; fax: +385 1 4590 236 (B. Foretić), tel.: +385 1 4566 755; fax: +385 1 4590 236 (I. Picek).
E-mail addresses: bforetic@mef.hr (B. Foretić), ipicek@mef.hr (I. Picek).

0277-5387/$ - see front matter © 2012 Elsevier Ltd. All rights reserved.
http://dx.doi.org/10.1016/j.poly.2012.07.077

and coordination properties still represent an important area of research in the view to recognize and rationalize relationships between the electronic/structural properties of the binding metal centers and the types of reactions they induce at the ligated aldoximes.

The low-spin pentacyano(ligand)ferrate(II) complexes, $[Fe(CN)_5(L)]^{n-}$, have been the subject of numerous investigations. They were found to be suitable as models for active sites in biological macromolecules [8], as representatives of supramolecular systems [9] and recently as electron donor groups for nonlinear optics [10]. Since the chemical properties of the $[Fe(CN)_5(L)]^{n-}$ are strongly dependent on the nature of L, the extensive characterization of *N*-heterocyclic and other *N*- and *S*-containing pentacyanoferrates(II) were summarized and reviewed [11]. Although the kinetics of a ligand substitution reactions with a wide variety of *N*-, *S*- and *O*-donor ligands were systematically and comprehensively studied providing the binding affinity of specific donors towards iron(II) [12], oximic ligands have never been among them. Thus, a comparative study concerning the coordination ability of the pyridinium-4-aldoxime containing ligands toward the pentacyanoferrate(II) moiety was performed, with a special regard to the *N*-methylpyridinium-4-aldoxime along with the two monopyridinium ligands and one bis-pyridinium ligand (Scheme 1). A detailed characterization of the *N*-methylpyridinium-4-aldoxime and its pentacyanoferrate(II) complex was performed using UV–Vis, NMR (^{1}H and ^{13}C), FT-IR spectral and thermal analysis, as well as X-ray diffraction in the case of the ligand. To recognize the chemical properties of the pyridinium-4-aldoxime pentacyanoferrate(II) complexes as well as the σ-donor and π-acceptor potential of the cited ligands, equilibrium and kinetic studies have been carried out.

2. Experimental

2.1. Materials and instruments

The starting materials for the synthesis of PAM4-I, BPA4-Cl·H_2O and FEPA4-Cl·H_2O were reagent grade products and employed as purchased. TMB4-2Br was obtained from Aldrich and purified before use. BPA4-Cl·H_2O and FEPA4-Cl·H_2O were synthesized according to a general procedure [5b]. Sodium amminepentacyanoferrate(II), $Na_3[Fe(CN)_5(NH_3)]\cdot 3H_2O$ (Sigma–Aldrich) was used after recrystallization from a concentrated ammonia solution. Solutions of $[Fe(CN)_5(H_2O)]^{3-}$ were obtained by aquation of $[Fe(CN)_5(NH_3)]^{3-}$ and were freshly prepared at room temperature and kept in the dark to minimize thermal and photolytic decomposition. The constant pH values of the aqueous solutions were maintained by using Britton and Robinson buffers, prepared by mixing 100 mL of phosphoric, boric and acetic acid solution (all 0.04 M) with different volumes of 0.2 M sodium hydroxide solution. A constant ionic strength was adjusted by the addition of sodium chloride. Redistilled water was used throughout. A pH-meter (Mettler Toledo) with an open junction combination polymer electrode was used for pH measurements accurate to ±0.01 pH units. Elemental analysis was performed with a LECO elemental analyzer, using the ASTM D 5291 method. Melting points were determined by a Stuart SMP3 apparatus with a temperature resolution of 0.1 °C. Thermal studies (TGA–DTA–DSC) were carried out in a N_2 atmosphere with the heating rate 5 °C min^{-1}. TA Instrument, Model SDT 2960 with a temperature range from 25 to 1600 °C was used for the TG–DT analysis. The DSC measurements were performed on TA Instrument, Model DSC 2910 with a temperature range from −150 to 725 °C.

The UV–Vis measurements were performed on either a UNICAM UV 4 or a Varian Cary Bio 100 spectrophotometer with thermostated cell holders and 1-cm silica-glass cells. FT-IR spectra were recorded on a Perkin Elmer Spectrum GX, Series R spectrometer in the range of 4000–400 cm^{-1} using KBr pellets. The ^{1}H and ^{13}C NMR spectra were recorded at room temperature with a Bruker AV-600 spectrometer equipped with 5 mm inverse detection or dual probes respectively, operating at 600.133 MHz for the ^{1}H nucleus and 150.917 MHz for the ^{13}C nucleus. The spectra were recorded in D_2O with tetramethylsilane as the internal standard.

2.2. TMB4-2Br and synthesis of $H[Fe(CN)_5(TMB4)]\cdot 2H_2O$

The commercially available TMB4-2Br was purified by recrystallization from ethanol according to known procedure [13]. The obtained pale yellow precipitate was analyzed by FT-IR and NMR spectroscopy. FT-IR (cm^{-1}): ν(O–H)$_{oxime}$, 3437 (vs); ν(C=N)$_{oxime}$, 1645 (vs); ν(C–C, C–N)$_{pyridinium\ ring}$, 1611 (vs), 1570 (m), 1521 (s); ν(NO), 1017 (vs), 984 (vs).

^{1}H NMR (D_2O, δ/ppm): 8.44 (s, H-1), 8.30 (d, J = 6.78 Hz, H-3(3′), H-6(6′)), 8.98 (d, J = 6.78 Hz, H-4(4′), H-5(5′)), 4.89 (t, J = 7.77 Hz, 2H-7(7′)), 2.91 (quin, J = 7.80 Hz, 2H-8). ^{13}C NMR (D_2O, δ/ppm): 146.3 (C-1(1′)), 149.2 (C-2(2′)), 125.9 (C-3(3′), C-6(6′)), 144.8 (C-4(4′), C-5(5′)), 57.8 (C-7(7′)), 31.7 (C-8). The chemical shifts were found to be in a good agreement with those published for TMB4-2Br in DMSO-d_6 [14].

The solid dark blue TMB4-pentacyanoferrate(II) complex was isolated as a precipitate from the aqueous mixture containing $[Fe(CN)_5(H_2O)]^{3-}$ and a fivefold excess of aldoxime at the

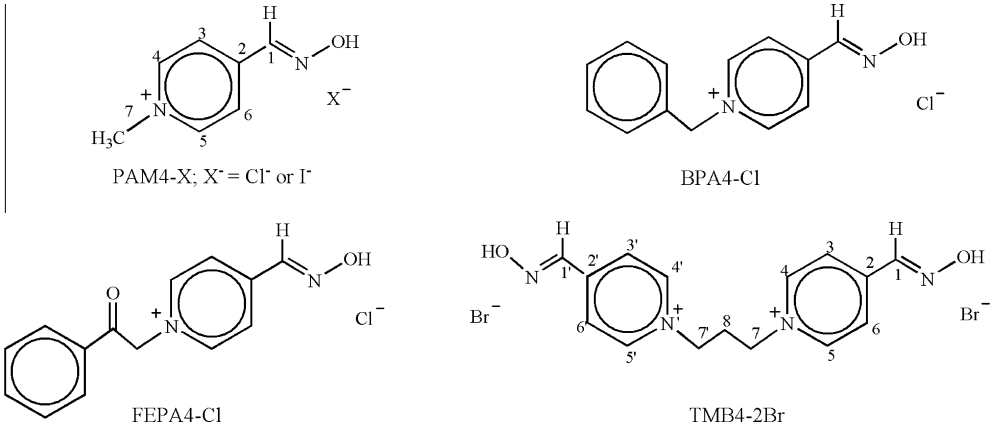

Scheme 1. Assignment of the ligands: *N*-methylpyridinium-4-aldoxime chloride (PAM4-Cl) and iodide (PAM4-I), *N*-benzylpyridinium-4-aldoxime chloride (BPA4-Cl), *N*-phenacylpyridinium-4-aldoxime chloride (FEPA4-Cl) and *N*,*N*′-bis(pyridinium-4-aldoxime)trimethylene dibromide (TMB4-2Br).

concentrations above 10^{-3} M and purified as described previously [4d]. *Anal.* Calc. for $H[Fe(CN)_5(C_{15}H_{18}N_4O_2)]\cdot 2H_2O$: C, 47.16; H, 4.55; N, 24.75; Fe, 10.97. Found: C, 47.24; H, 4.59; N, 24.60; Fe, 10.86%.

FT-IR (cm^{-1}): $\nu(O–H)_{water}$ + $\nu(O–H)_{oxime}$, 3402 (br, s); $\nu(CN)_{cyano}$, 2108 (m), 2044 (vs); $\nu(C{=}N)_{oxime\ free}$ + $\nu(C{=}N)_{oxime\ bonded}$, 1643 (br, vs) + 1637 (sh, vs); δ(HOH), 1616 (s); $\nu(C–C, C–N)_{pyridinium\ ring}$, 1611 (s), 1576 (s), 1517 (vs); $\nu(NO)_{free}$ + $\nu(NO)_{bounded}$, 1013 (br, vs).

2.3. Synthesis of PAM4-I and PAM4-Cl·H_2O single crystals

PAM4-I was prepared according to a general procedure by mixing ethanol solution of pyridine-4-aldoxime (Fluka) with iodomethane (Sigma–Aldrich) present in threefold excess. The resulting mixture was stirred at room temperature for 1 day. The produced crystalline precipitate was filtered off and purified by recrystallization from ethanol. Yellow, water-soluble single crystals of PAM4-I were obtained (m.p.: 170.5 °C, decomp.). Yield, 47%. *Anal.* Calc. for $C_7H_9N_2OI$: C, 31.84; H, 3.44; N, 10.61. Found: C, 31.89; H, 3.41; N, 10.70%. FT-IR (cm^{-1}): $\nu(O–H)_{oxime}$, ~3150 (s); $\nu(C{=}N)_{oxime}$, 1644 (s); $\nu(C–C, C–N)_{pyridinium\ ring}$, 1611 (s), 1573 (w), 1520 (m); ν(NO), 1000 (vs).

^{1}H NMR (D_2O, δ/ppm): 8.51 (s, H-1), 8.32 (d, J = 6.60 Hz, H-3, H-6), 8.91 (d, J = 6.66 Hz, H-4, H-5), 4.52 (s, 3H-7). ^{13}C NMR (D_2O, δ/ppm): 145.3 (C-1), 148.4 (C-2), 124.3 (C-3, C-6), 145.0 (C-4, C-5), 47.9 (C-7).

PAM4-I was converted into corresponding chloride by treatment with methanolic solution of hydrogen chloride in accordance with a convenient method of anion exchange in quaternary salts [15]. PAM4-I was dissolved in freshly prepared methanolic solution saturated with anhydrous HCl at room temperature. The solution was concentrated by evaporation under reduced pressure followed by addition of acetone and allowed to cool in a refrigerator (at 4 °C). After 2 days, the produced transparent crystals of monohydrate salt, PAM4-Cl·H_2O, were filtered off, washed with acetone and dried in vacuum (m.p.: 169.1 °C, decomp.). Yield, 42%. *Anal.* Calc. for $C_7H_{11}N_2O_2Cl$: C, 44.10; H, 5.81; N, 14.70. Found: C, 44.09; H, 5.61; N, 14.71%. FT-IR (cm^{-1}): $\nu(O–H)_{water}$ + $\nu(O–H)_{oxime}$, 3356 (s), 3216 (s); $\nu(C{=}N)_{oxime}$, 1639 (s); $\nu(C–C, C–N)_{pyridinium\ ring}$, 1607 (s), 1567 (m), 1519 (vs); ν(NO), 1008 (vs).

^{1}H NMR (D_2O, δ/ppm): 8.46 (s, H-1), 8.30 (d, J = 6.54 Hz, H-3, H-6), 8.92 (d, J = 6.54 Hz, H-4, H-5), 4.54 (s, 3H-7). ^{13}C NMR (D_2O, δ/ppm): 145.9 (C-1), 147.7 (C-2), 124.2 (C-3, C-6), 145.0 (C-4, C-5), 47.6 (C-7).

2.3.1. X-ray single-crystal structure determination

Diffraction data were collected from suitable single crystals of PAM4-I-o (orthorhombic polymorph) and PAM4-Cl·H_2O on an Oxford Diffraction Xcalibur single-crystal diffractometer with Xcalibur Sapphire 3 CCD detector and Mo Kα radiation. The CrysAlis Software system, Version 171.32.24 [16] was used for data collection and reduction. Data for PAM4-I-o were collected at room temperature (296 K) while those for PAM4-Cl·H_2O were collected at low temperature (150 K). Later, the crystals of PAM4-I obtained directly from the reaction were remeasured at 150 K (same diffractometer) but it was found to be a different polymorph (monoclinic) and will be referred to as PAM4-I-m. All trials to obtain again the orthorhombic polymorph have failed so far. It was difficult to find a single crystal of PAM4-I-m because of twinning. The measured crystal also had 7% of the twin component (twin law (001)[104]) however since the structure refined well the small twin component was not used in calculations. The unit cell of PAM4-I-m was checked at room temperature to test if there is a possible phase transition due to the change in temperature. The obtained unit cell (a = 7.112(6) Å, b = 10.403(6) Å, c = 13.303(14) Å, β = 95.58(7)°) shows no transformation to PAM4-I-o. The multi-scan procedure was used for absorption effects. The structures were solved by direct methods with SHELXS-97 [17]. Refinement procedure by the full-matrix least squares method based on F^2 values against all reflections was performed. Anisotropic displacement parameters for all non-hydrogen atoms were included.

The positions of hydrogen atoms belonging to the carbon atoms Csp^2 and methyl Csp^3 atoms were geometrically optimized in all three structures applying the riding model [Csp^2–H, Csp^3 (methyl)–H, 0.93 Å and 0.96 Å, respectively; $U_{iso}(H) = 1.2U_{eq}(C)$ for Csp^2 and $1.5U_{eq}(C)$ for Csp^3(methyl)]. The hydrogen atom belonging to the oxime O1 atom in PAM4-I-o was not found in the difference Fourier map, nor could its position be modeled by applying the appropriate riding model. In the structure of PAM4-Cl·H_2O, all hydrogen atoms were located in the difference Fourier maps however those on the C-atoms were geometrically optimized. Those on the oxime O1 and on the water molecule were placed as found in the map and were refined isotropically. In PAM4-I-m the oxime hydrogen atom was calculated as an idealized hydroxyl group with the torsion angle from the electron density. Calculations were performed with SHELXL-97 [17], PLATON [18] and PARST [19]. The molecular graphics were done with PLATON and MERCURY (Version 1.4.2) [20]. Crystal data and details of the structure determination for PAM4-I polymorphs and PAM4-Cl·H_2O are given in Table 1.

2.4. Synthesis of Na(PAM4)[Fe(CN)$_5$(PAM4)]·H_2O

PAM4-I, dissolved in the minimal volume of ethanol–water solution (in volume ratio of approx. 1) was added to the concentrated aquated $[Fe(CN)_5(NH_3)]^{3-}$ solution in fivefold excess. The instantly produced dark blue reaction mixture was kept in the refrigerator overnight (at 4 °C). Afterwards, the precipitation was initiated by addition of ethanol. The produced dark-blue powder was filtered off, washed with ethanol and dried in vacuum. Yield, 26%. *Anal.* Calc. for $Na(C_7H_9N_2O)[Fe(CN)_5(C_7H_9N_2O)]\cdot H_2O$: C, 45.53; H, 4.02; N, 25.15. Found: C, 45.10; H, 4.39; N, 24.71%. TGA analysis supported the loss of one water molecule upon heating. Unfortunately, attempts to obtain crystals of complex suitable for X-ray structural analysis remained unsuccessful. FT-IR (cm^{-1}): $\nu(O–H)_{water}$ + $\nu(O–H)_{oxime}$, 3400 (br, vs); $\nu(CN)_{cyano}$, 2111 (s), 2057 (vs); $\nu(C{=}N)_{oxime\ free}$ + $\nu(C{=}N)_{oxime\ bounded}$, 1643 (br, vs); $\nu(C–C, C–N)_{pyridinium\ ring}$, 1614 (vs), 1573 (s), 1522 (vs); $\nu(NO)_{free}$ + $\nu(NO)_{bounded}$, 1009 (br, vs).

The ^{1}H and ^{13}C NMR spectra were taken immediately after dissolving the complex in D_2O. In the ^{1}H NMR spectrum only the broad signals with the absence of the expected splitting patterns were observed. ^{13}C NMR shifts of coordinated and uncoordinated PAM-4 were distinguishable except for the signals corresponding to the C-2 and C-4, C-5 atoms. ^{13}C NMR (D_2O, δ/ppm) of the complex anion: 149.6 (C-1), 128.2 (C-3, C-6), 48.1 (C-7), 173.2 (*cis*-C≡N), 169.0 (*trans*-C≡N).

2.5. Electronic absorption studies

2.5.1. Determination of the PAM4-I and PAM4-Cl ionization constants

The spectrophotometric titrations of the 4×10^{-5} M solutions of PAM4-I and PAM4-Cl were performed at 25 °C and I = 0.1 M. The spectral characteristics of the respective ionic forms and the ionization constants were derived from the absorbance versus pH curves by a non-linear regression as described previously [5] (Fig. S1).

2.5.2. Determination of the apparent formation constants for $[Fe(CN)_5(H_nL)]^{(3-n)-}$ complexes

Equilibrium constants specified as apparent formation constants, β_f, have been evaluated by non-linear regression of the

Table 1
Crystal data and details of the structure determination for PAM4-I-o and PAM4-I-m polymorphs and PAM4-Cl·H_2O.

Compound	**PAM4-I-o**	**PAM4-I-m**	**PAM4-Cl·H_2O**
Empirical formula	$C_7H_9IN_2O$	$C_7H_9IN_2O$	$C_7H_{11}ClN_2O_2$
M_r	264.06	264.06	190.63
Color and habit	yellow, prism	yellow, prism	colorless, prism
Crystal system	orthorhombic	monoclinic	orthorhombic
Space group	*Pnam*	$P2_1/c$	$P2_12_12_1$
Crystal dimensions (mm)	0.70 × 0.39 × 0.30	0.51 × 0.37 × 0.25	0.44 × 0.40 × 0.23
Unit cell parameters			
a (Å)	13.2260(12)	7.0204(3)	6.80810(10)
b (Å)	10.4618(8)	10.3580(4)	8.9236(2)
c (Å)	7.0852(7)	13.2217(5)	14.5295(3)
α (°)	90	90	90
β (°)	90	98.150(4)	90
γ (°)	90	90	90
V (Å^3)	980.36(15)	951.74(7)	882.71(3)
Radiation, Mo Kα (Å)	0.71073	0.71073	0.71073
Z	4	4	4
D_{calc} (g cm^{-3})	1.789	1.843	1.434
μ (mm^{-1})	3.218	3.315	0.394
θ range for data collection (°)	3.80–26.99	4.23–29.00	4.57–30.00
h, k, l range	−16:16; −13:13, −9:9	−9:9; −12:14; −18:18	−4:9; −10:12; −20:16
Number of measured reflections	21902	4786	4482
Number of independent reflections (R_{int})	1155 (0.0357)	2481 (0.0139)	2555 (0.0113)
Number of observed reflections, $I \geqslant 2\sigma(I)$	1081	2246	2511
Number of refined parameters	68	126	126
R,[a] wR[b] [$I \geqslant 2\sigma(I)$]	0.0497, 0.1426	0.0431, 0.1083	0.0243, 0.0626
R, wR [all data]	0.0544, 0.1464	0.0470, 0.1100	0.0252, 0.0636
g_1, g_2 in w[c]	0.0758, 1.0496	0.0243, 7.9293	0.0403, 0.0566
Flack parameter	–	–	0.00(4)
Goodness of fit on F^2, S[d]	1.210	1.199	0.989
Maximum, minimum electron density (e Å^{-3})	1.028, −0.368	−1.080, 2.149	0.204, −0.181
Maximum Δ/σ	<0.001	<0.001	<0.001
Absorption correction type	multi-scan	multi-scan	multi-scan
Range of transmission factors minimum, maximum	0.240, 0.380	0.744, 1.000	0.921, 1.000

[a] $R = \Sigma||F_o| - |F_c||/\Sigma|F_o|$.
[b] $wR = [\Sigma(F_o^2 - F_c^2)^2/\Sigma w(F_o^2)2]1^{/2}$.
[c] $w = 1/[\sigma^2(F_o^2) + (g_1P)^2 + g_2P]$ where $P = (F_o^2 + 2F_c^2)/3$.
[d] $S = \Sigma[w(F_o^2 - F_c^2)^2/(N_{obs} - N_{param})]^{1/2}$.

experimental data to the hyperbolic Eq. (1) valid for the spectrophotometric mole ratio method [21].

$$A_{\lambda(\mathrm{MLCT})} = \frac{1}{2}A_{\mathrm{lim}} \cdot \left(1 + z + \frac{1}{\beta_f \cdot c([Fe(CN)_5(H_2O)]^{3-})} - \sqrt{\left(1 + z + \frac{1}{\beta_f \cdot c([Fe(CN)_5(H_2O)]^{3-})}\right)^2 - 4 \cdot z}\right) \quad (1)$$

Absorbances collected at the metal-to-ligand charge transfer (MLCT) maximum of the formed complexes at 25 °C, I = 0.1 M and pH 6.04 ± 0.02 were analyzed (Fig. S2). The mole ratio of ligand to metal analytical concentrations is defined by parameter z with the constant total analytical concentration of $[Fe(CN)_5(H_2O)]^{3-}$ (2×10^{-4} M) through measurements and A_{lim} is theoretical absorbance corresponding to quantitative reaction:

$$z = \frac{c(H_nL^{n+})}{c([Fe(CN)_5(H_2O)]^{3-})};$$

$$A_{\mathrm{lim}} = \varepsilon([Fe(CN)_5(H_nL)]^{(3-n)-}) \cdot c([Fe(CN)_5(H_2O)]^{3-}).$$

2.5.3. Kinetic measurements

The formation rates of $[Fe(CN)_5(H_nL)]^{(3-n)-}$ complexes were measured spectrophotometrically at the wavelengths corresponding to the MLCT bands of the complexes at 25.0 ± 0.5 °C, I = 0.1 M and pH 6.0 ± 0.2. The pseudo-first-order rate constants, k_{obs}, were obtained from the slopes of the linear least-squares fits of $\ln(A_\infty - A_t)$ versus time plots, where A_t is the absorbance at time t and A_∞ is the maximal absorbance reached during the course of the reaction. In all the kinetic solutions the concentration of $[Fe(CN)_5(H_2O)]^{3-}$ was 5×10^{-5} M. The data were collected under pseudo-first-order conditions by the use of a 20- to 150-fold molar excess of the ligand. All measurements were performed in triplicate. The second-order formation rate constant, k_f, was obtained as the slope of a plot of k_{obs} versus the concentration of the ligand (Fig. S3).

The dissociation kinetic study of $[Fe(CN)_5(H_nL)]^{(3-n)-}$ complexes was performed under pseudo-first-order conditions by following the absorbance decrease at the wavelengths corresponding to the MLCT maximum of the formed complexes after addition of large excess of DMSO as a $[Fe(CN)_5(H_2O)]^{3-}$ scavenger. The quantitative formation of $[Fe(CN)_5(H_nL)]^{(3-n)-}$ in initial reaction mixtures was ensured by the addition of 25-fold excess of ligands to a 5×10^{-5} M $[Fe(CN)_5(H_2O)]^{3-}$ solutions. The pseudo-first-order rate constant, identified as k_d, was determined from the dependence of $\ln(A_t)$ versus time. All measurements were performed in triplicate and pH range from 5.0 to 11.5. The thermal activation parameters for the dissociation reactions were determined at pH 6.0 from the Eyring linear plots of $\ln[(k_d/T)/(s^{-1}\,K^{-1})]$ versus $1/T$ within the temperature range 10–30 °C.

3. Results and discussion

3.1. The crystal structures of PAM4-Cl·H_2O, PAM4-I-o and PAM4-I-m

ORTEP view of the molecular structures of PAM4-Cl·H_2O and PAM4-I-m is depicted in Fig. 1. That of PAM4-I-o is given in the

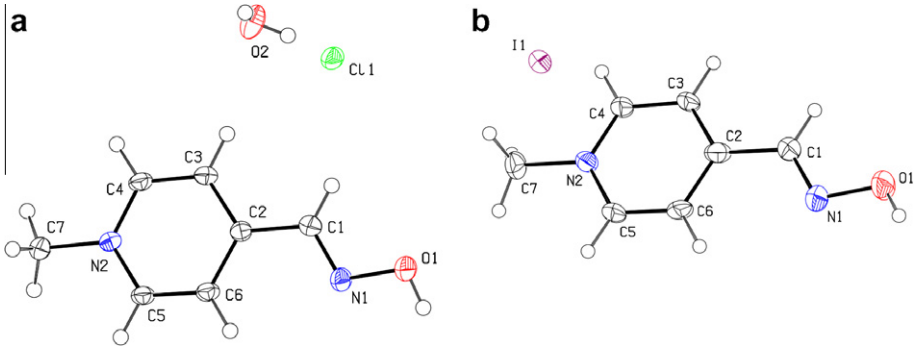

Fig. 1. ORTEP drawing of (a) PAM4-Cl·H_2O and (b) PAM4-I-m with the atom numbering scheme. Thermal ellipsoids are shown at the 50 probability level at 150 K.

Fig. S4. The crystal structures of PAM4-I polymorphs are given in the Fig. S5. The asymmetric unit of PAM4-Cl·H_2O contains a *N*-methylpyridinium-4-aldoxime cation, a chloride ion and a water molecule of crystallization (Fig. S5). The selected molecular geometry parameters for all three structures are listed in Table 2 and hydrogen bond geometry in the Table S1. The bond distances and angles in the structure of PAM4-I polymorphs and PAM4-Cl·H_2O correspond well to the values found in the literature for similar structures containing the aldoxime moiety bonded to the pyridinium ring in the position 4 (Table 2) [5a,22,23]. The arrangement of substituents around the C=N bond in all three structures shows that the aldoxime has the *E*-configuration (Fig. 1 and Fig. S4). The value of the endocyclic bond angle C4–N2–C5 deviates from the ideal value for the six-membered ring by 0.2(8)° (PAM4-I-o), 1.0(5)° (PAM4-I-m) and 0.8(1)° (PAM4-Cl·H_2O). This deviation is significantly smaller than the ones found for pyridoxal oxime methyl iodide (2.5(3)°) and for pyridoxal oxime methyl chloride (2.2(1)°) [23a]. The sum of the endocyclic bond angles is 720° as it is expected for an unpuckered aromatic ring. The conformation of the aldoxime moiety is antiperiplanar, while the torsion angle O1–N1–C1–C2 is 179.23(9)° in PAM4-Cl·H_2O, 180° in PAM4-I-o and 179.7(6)° in PAM4-I-m. The pyridinium ring in PAM4-I-o does not deviate from planarity since the whole molecule (including the iodide anion) lies on a crystallographic mirror plane, while in PAM4-I-m the molecule is in the general position and the greatest deviation from the plane through the pyridinium ring is 0.151(6) Å of atom O1. In PAM4-Cl·H_2O the greatest deviation is 0.124(1) Å of the N1 atom. There is a hydrogen bond O1–H···I between the *N*-methylpyridinium-4-aldoxime cation and the iodide anion in the crystal structures of the two PAM4-I polymorphs (Fig. S5). Similar O–H···Br hydrogen bond was found between *N*-benzylpyridinium-4-aldoxime cation and bromide anion in the crystal structure of *N*-benzylpyridinium-4-aldoxime bromide [23b]. In the structure of PAM4-Cl·H_2O the water molecule links the chloride anions and PAM4 cations into endless chains parallel to [100]. Two hydrogen bonds of the O–H···Cl type are observed (Fig. S5 and Table S1) with a water molecule being a bridging hydrogen bond donor toward two chloride anions. In addition, the water molecule is an acceptor of a hydrogen bond from the aldoxime hydroxyl group. In the three structures there are also weak intermolecular hydrogen bonds of the C–H···O type. Furthermore, the crystal packing of PAM4-I and PAM4-Cl·H_2O is stabilized by intermolecular C–H···I and C–H···Cl contacts, respectively. These interactions in the structure of PAM4-I link the *N*-methylpyridinium-4-aldoxime cations and iodide anions into a network parallel to (001). These networks are further assembled in the [001] direction only by weak van der Waals interactions.

Table 2
Selected bond distances (Å) and angles (°) for PAM4-I-o and PAM4-I-m polymorphs and PAM4-Cl·H_2O.

Compound	PAM4-I-o	PAM4-I-m	PAM4-Cl·H_2O
N1–C1	1.354(16)	1.275(8)	1.2802(14)
C1–C2	1.456(14)	1.476(8)	1.4669(15)
C2–C3	1.376(12)	1.361(8)	1.4008(14)
C2–C6	1.369(15)	1.398(9)	1.3990(14)
C3–C4	1.373(13)	1.383(8)	1.3760(15)
C4–N2	1.312(10)	1.325(7)	1.3518(13)
C5–N2	1.319(11)	1.344(7)	1.3446(13)
C5–C6	1.358(14)	1.376(9)	1.3767(15)
C7–N2	1.467(11)	1.474(7)	1.4779(14)
N1–O1	1.287(13)	1.375(7)	1.3816(12)
O1–N1–C1	105.0(14)	111.0(5)	112.40(9)
N1–C1–C2	114.9(9)	120.1(6)	117.23(9)
C3–C2–C1	118.8(9)	120.8(6)	120.83(10)
C6–C2–C1	123.6(8)	120.3(5)	121.19(10)
C3–C2–C6	117.6(9)	118.8(6)	117.97(9)
C4–C3–C2	119.1(8)	119.8(5)	119.84(10)
N2–C4–C3	121.6(8)	120.8(5)	120.59(10)
N2–C5–C6	121.0(8)	120.4(5)	120.95(10)
C5–C6–C2	120.4(8)	119.2(5)	119.80(10)
C5–N2–C4	120.2(8)	121.0(5)	120.76(9)
C4–N2–C7	120.9(8)	119.5(5)	120.91(9)
C5–N2–C7	119.0(8)	119.5(5)	118.31(9)

3.2. Spectroscopic and thermal studies

3.2.1. Spectroscopic studies of PAM4-I and PAM4-Cl·H_2O

The electronic absorption spectra of PAM4-Cl and PAM4-I were recorded in aqueous solutions in the pH range of 5.0–11.5. The two intensive pH-dependent bands at about 280 and 340 nm were observed, typical for the $\pi \rightarrow \pi^*$ transitions within the protonated and deprotonated pyridinium-4-aldoxime system, respectively, as was previously found for the solutions of BPA4-Cl, FEPA4-Cl and TMB4-2Br [5b,24]. However, the low intensity band centered on 240 nm attributed to the deprotonated pyridinium-4-aldoxime chromophore, was observed only in the absorption spectra of PAM4-Cl. In the spectra of PAM4-I this band was covered by intensive, pH-independent charge-transfer band with a maximum around 225 nm. Like in a similar electronic system, present in *N*-methylpyridinium iodide, the band arose as a consequence of the $PAM4^+I^-$ association complex formation predominantly driven by electrostatic forces [25]. To eliminate the possible influence of such association on ionization properties and reactivity of the pyridinium-4-aldoxime group the ionization constants of both, PAM4-Cl and PAM4-I, were determined and the ^1H and ^{13}C NMR spectra in D_2O were correlated. The comparative UV–Vis spectroscopic characterization of the respective ionic forms and the ionization constants of the pyridinium-4-aldoxime group in the examined ligands are presented in Table 3. In view of the fact that the ionization of the carbonyl group in FEPA4 ion was negligible in specified pH range [5], it was treated as mono-pyridinium-4-aldoxime.

Table 3
The ionization constants and molar absorption coefficients of the predominant ionic forms of the pyridinium-4-aldoximic compounds in aqueous solutions at 25 °C and $c = 4 \times 10^{-5}$ M.

Compound	λ_{max} (nm)	$\varepsilon(H_2L^{2+})_{max}$ (M^{-1} cm^{-1})	$\varepsilon(HL^{+})_{max}$ (M^{-1} cm^{-1})	$\varepsilon(L)_{max}$ (M^{-1} cm^{-1})	$pK_{a1(aldoxime)}$	$pK_{a2(aldoxime)}$
PAM4-I[a]	279		18330	3440	8.56 ± 0.05	
	337			25860		
PAM4-Cl·H_2O[a]	278		15990	2800	8.57 ± 0.05	
	336			22270		
BPA4-Cl·H_2O[b]	283		16194		8.76 ± 0.02	
	342			24280		
FEPA4-Cl·H_2O[b]	283		23330		8.72 ± 0.07	
	345			27800		
TMB4-2Br[c]	282	41200	29890	5600	7.50 ± 0.08	8.90 ± 0.08
	345		22660	54130		

[a] This work: $I = 0.1$ M.
[b] Data from Ref. [5b]: $I = 0.1$ M.
[c] Data from Ref. [24]: $I = 0.05$ M.

The identical values of ionization constants for PAM4-I and PAM4-Cl (close to the literature pK_a value of 8.44 [26]) as well as the negligible differences in the NMR chemical shifts were established. In addition, the NMR chemical shifts were in a good agreement with those obtained for the TMB4-2Br (see Section 2), BPA4-Cl and FEPA4-Cl [5b]. This clearly indicated a negligible impact of the $PAM4^+I^-$ association complex formation to PAM4 reactivity towards the $[Fe(CN)_5]^{3-}$ moiety.

The similar acidities of the pyridinium-4-aldoxime moieties in the examined compounds were found to be in accordance with the similar positions and intensities of the aldoximic C=N and N–O stretching frequencies in the IR spectra (see Section 2). The higher frequencies of N–O stretching accompanied by lower C=N frequencies when compared with the frequencies in pyridine-4-aldoxime revealed the considerable resonance contribution of =C–N=O^+–H [27]. Evidently, the ionization abilities of mono- and bis-pyridinium-4-aldoximes were essentially independent of the substituent attached to the *N*-methylenepyridinium moiety. Although the mean pK_a value of 8.2 that has been established for the bis-pyridinium-4-aldoxime, TMB4, fits well, the difference between pK_{a1} and pK_{a2} ($\Delta pK_a \sim 1.4$) implies that ionization of the first aldoxime group influences the ionization of the second. The pK_a difference in the range of 0.6–0.7, based solely on statistical factors, was shown earlier for some symmetric bis-pyridinium aldoximes [26] and was in agreement with a lack of direct electronic communication between the two pyridinium aldoximic donor sites. Therefore, in symmetrically structured TMB4, without possibility of an electronic communication between the two pyridinium-4-aldoxime rings, the indicated effect may be associated only with the steric disturbances.

3.2.2. Spectroscopic studies of $Na(PAM4)[Fe(CN)_5(PAM4)]\cdot H_2O$

The solids of the pentacyanoferrates(II) complexed with monopyridinium-4-aldoximes, PAM4 and formerly described BPA4 and FEPA4, have been water-soluble to some extent, while the complex with bis-pyridinium-4-aldoxime, TMB4, has been insoluble. The pH-dependent UV–Vis spectra of the solutions of the newly synthesized $Na(PAM4)[Fe(CN)_5(PAM4)]\cdot H_2O$ solid are presented in Fig. 2. The UV region was dominated by the intensive superimposed intraligand absorption bands due to $\pi \rightarrow \pi^*$ transitions within the uncoordinated and coordinated ligand ($\lambda_{max} \sim 282$ nm, $(\varepsilon(HL^+) + \varepsilon([Fe(CN)_5(HL)]^{2-}))_{max} = 30900\ M^{-1}\ cm^{-1}$; $\lambda_{max} \sim 340$ nm, $(\varepsilon(L) + \varepsilon([Fe(CN)_5(L)]^{3-}))_{max} = 35550\ M^{-1}\ cm^{-1}$), whose intensity was pH-dependent. These pH-dependent spectral changes exhibited excellent isobesticity. The dependence of absorbances at these maxima on pH resulted in clear titration curves (inset in Fig. 2) whose inflection points revealed the pK_a value higher than 8.6 established for free PAM4, and thus proving the expected significant contribution of coordinated PAM4 as extended chromophore. The low intensity band due to $^1A_1 \rightarrow {}^1E(1)$ *d–d* transition, usually positioned in the range from 264 to 444 nm [11a,12h], which has been found to be sensitive to the nature of the sixth ligand for a large number of pentacyano(ligand)ferrate(II) complexes was completely masked. In the visible region, characteristic broad, intensive maximum centered in the range from 560 to 570 nm was compatible with the metal-to-ligand charge transfer, $t_{2g} \rightarrow L_{\pi*}$, whose energy, and only slightly intensity, was pH-sensitive ($\varepsilon = 4830 \pm 530\ M^{-1}\ cm^{-1}$). The MLCT band shifted about 10 nm toward lower energy upon increasing the pH of the medium over 9, due to the equilibrium:

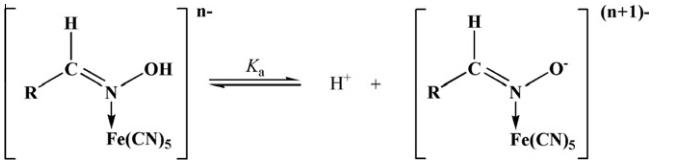

(2)

where R represents the pyridinium part of the ligand. Similar red-shifts in the MLCT band together with small intensity changes were noted previously for the complexes produced with BPA4 and FEPA4 [5b] and were also observed for the aqueous reaction mixtures of the TMB4-pentacyanoferrate(II). These decreases in the MLCT energy are attributable to increases in the electron density at the iron(II) center caused by deprotonation of the coordinated ligand.

The ^{13}C NMR spectrum of the PAM4-pentacyanoferrate(II) contained two sets of signals corresponding to C-1, C-3,6 and C-8 nuclei of both the coordinated and uncoordinated PAM4. Furthermore, two cyanide resonance signals, with a ratio of relative intensities of 4:1, were assigned to four *cis*- (173.2 ppm) and one *trans*-configured cyano groups (169.0 ppm) and are consistent with the *trans*-configuration of PAM4 in the octahedral PAM4-pentacyanoferrate(II). The upfield shifts of the *cis*- and *trans*-cyano groups in respect to hexacyanoferrate(II) ion (177 ppm) [11a], also observed for the BPA4-pentacyanoferrate(II) [5b] were evident. The shielding of the cyano carbon atoms is most probably the result of increased π-back donation from iron(II) to cyano ligands due to pronounced σ-induction of electron density from coordinated PAM4 towards iron(II). This is strongly supported by the considerable deshielding of aldoxime carbon atom as a consequence of the increased polarization of the aldoxime C=N bond which is consistent with the poor π-acceptor ability of the coordinated PAM4.

The FT-IR spectra of PAM4-Cl·H_2O, PAM4-I and TMB4-2Br, similar to the previously characterized BPA4-Cl·H_2O and FEPA4-Cl·H_2O, exhibit strong bands due to aldoxime C=N and N–O stretchings at ca. 1643 cm^{-1} and 1000 cm^{-1}, respectively. Generally, upon

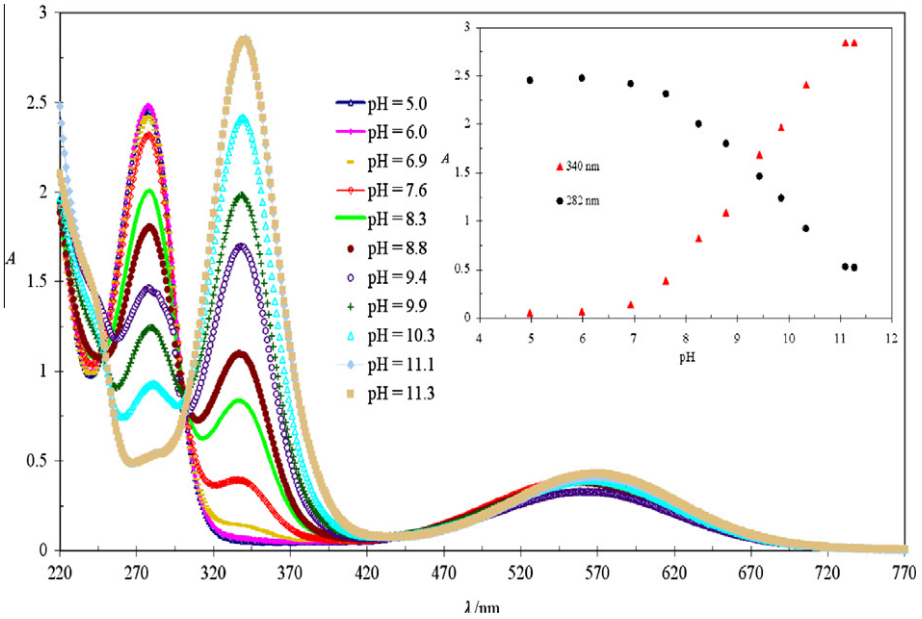

Fig. 2. pH-dependent UV–Vis spectra of the isolated Na(PAM4)[Fe(CN)$_5$(PAM4)]·H$_2$O in aqueous solutions at 25 °C, $c = 8 \times 10^{-5}$ M, $I = 0.1$ M.

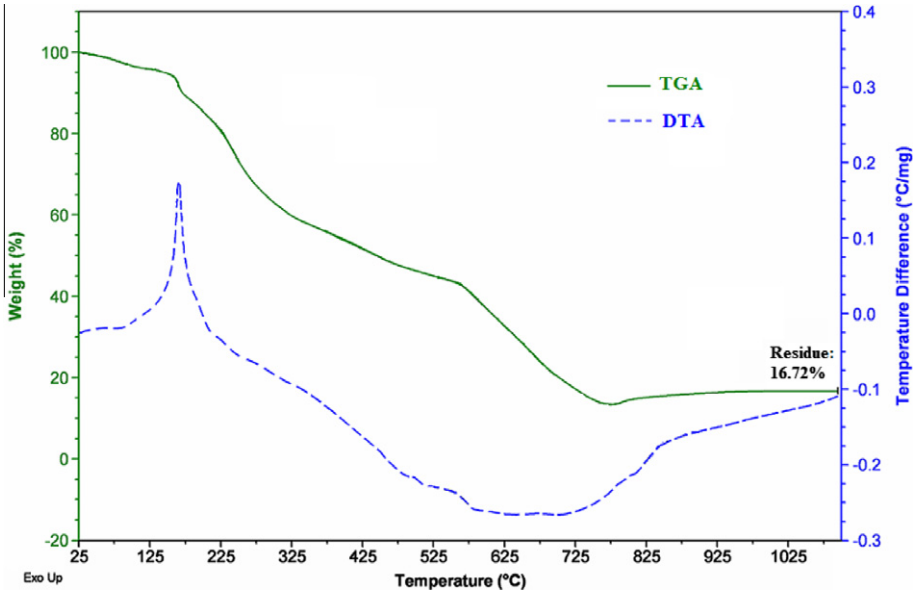

Fig. 3. TGA and DTA curves for Na(PAM4)[Fe(CN)$_5$(PAM4)]·H$_2$O.

coordination of the oxime nitrogen to a metal ion the C=N stretches shift to lower frequencies, while N–O stretches shift toward higher frequencies [28]. This is not pronounced in the spectra of the pyridinium-4-aldoxime pentacyanoferrate(II) complexes. Despite the strong absorption of the uncoordinated mono-pyridinium-4-aldoximes (PAM4, BPA4, FEPA4) present as cationic counterparts, as well as the uncoordinated *N*-methylenepyridinium-4-aldoxime part in the bis-pyridinium-4-aldoxime (TMB4), only the broadening of the N–O stretching bands in the examined pentacyanoferrate(II) complexes points to the coordination. Therefore, only the cyanide stretching modes, in the 2100–2000 cm^{-1} range, has been found as diagnostically valuable. Their similar positions and the splitting pattern are found in the spectra of all examined pyridinium-4-aldoxime pentacyanoferrates(II) (this work: PAM4, TMB4; in Ref. [5b]: BPA4, FEPA4). They are distinctive for the octahedral pentacyano(ligand)ferrate(II) complexes [11a,29] and strongly indicate the analogous mode of coordination emphasizing the same nature of the formed iron(II)–pyridinium-4-aldoxime bond. The striking similarity between the spectra of the complexes to those of free ligands suggest that σ- and π-bonding effects seem nearly to cancel out, as was the case for pentacyanoferrates(II) complexed with pyridyl amide derivatives [30].

3.2.3. Thermal behavior of Na(PAM4)[Fe(CN)$_5$(PAM4)]·H$_2$O

The TGA, DTA and DSC curves (Fig. 3 and Fig. S6) revealed multistage decomposition of the PAM4-pentacyanoferrate(II) in a similar manner as observed for other pentacyano(ligand)ferrates(II) [31]. The decomposition started around 30 °C and ended at 750 °C yielding a final stable product with 16.72% of residual weight. In initial stage, upon heating the sample up to 100 °C, where generally the dehydration occurs [31], the endothermic process was observed with the total weight loss of 3.70%. This is in

Table 4
Formation kinetics and equilibrium constants of $[Fe(CN)_5(H_nL)]^{(3-n)-}$ at 25.0 ± 0.5 °C and I = 0.1 M.

Complex	λ_{MLCT} (nm)	$\log(\beta_f/M^{-1})$	k_f (M^{-1} s^{-1})	$\log[(k_f/k_d)/M^{-1}]$
$[Fe(CN)_5(PAM4)]^{2-}$	560	1.91	3.9 ± 0.3	2.44
$[Fe(CN)_5(BPA4)]^{2-}$	574	2.54	7.6 ± 0.2	2.74
$[Fe(CN)_5(FEPA4)]^{2-}$	580	2.16	4.1 ± 0.4	2.53
$[Fe(CN)_5(TMB4)]^{-}$	575	2.62	19.7 ± 0.5	3.15

accordance with the release of one water molecule (theoretical: 3.60%) and confirms that within the isolated complex mole ratio $Na(PAM4)[Fe(CN)_5(PAM4)]/H_2O$ equals to 1. The next decomposition stages in the temperature ranges of 94–220 °C and 270–520 °C, evidenced by two exothermic peaks in DTA and DSC curves, clearly indicated the simultaneous decomposition reactions which could not be resolved. Thus, the clear release of coordinated and uncoordinated PAM4 was not observed. The total weight loss of 83.28% was in good agreement with the weight loss corresponding to the loss of one water molecule, two PAM4 cations and five cyanide groups (theoretical: 84.26%) and strongly supported the proposed molecular formula of the isolated complex.

3.3. Equilibrium and kinetic studies

The substitution of water in the $[Fe(CN)_5(H_2O)]^{3-}$ with the pyridinium-4-aldoximic ligands is presented by the following general equation with a related equilibrium constant:

$$[Fe(CN)_5(H_2O)]^{3-} + H_nL^{n+} \underset{k_d}{\overset{k_f}{\rightleftarrows}} [Fe(CN)_5(H_nL)]^{(3-n)-} + H_2O$$

$$\beta_f = \frac{[[Fe(CN)_5(H_nL)]^{(3-n)-}]}{[[Fe(CN)_5(H_2O)]^{3-}] \cdot [H_nL^{n+}]} \quad (3)$$

where n is an integer ranging from 1 to 0 for PAM4, BPA4 and FEPA4, and from 2 to 0 for TMB4.

For all examined ligands the spectrophotometric mole ratio method, performed at pH 6.04 ± 0.02, confirmed the formation of a complex of 1:1 molar composition and formation of the corresponding pentacyanoferrate(II) with a protonated pyridinium-4-aldoxime ligand, obviously bounded to the iron center via aldoximic nitrogen atom. Deduced equilibrium constants, specified as apparent formation constants, β_f, are presented in Table 4. Despite the smaller stabilities of the BPA4-, FEPA4- and TMB4-pentacyanoferrate(II) complexes that we have determined, when compared with the previous literature [4c,d], the apparent stabilities of the formed complexes are in good correlation with their kinetic properties. The comparison of stability constants with the literature values for various pentacyanoferrates(II) indicated the behaving of protonated pyridinium-4-aldoximes as weak π-acceptors [12a–c,g,h,j,k]. Similar MLCT energies of the formed pentacyanoferrates(II) suggested the analogous changes in electron distribution within the pyridinium ring upon coordination.

The ligand substitution reactions of water in labile $[Fe(CN)_5(H_2O)]^{3-}$ with a wide variety of entering ligands (forward reaction in Eq. (3)) have been shown to follow a dissociative mechanism [11]. Consequently, the formation rate has been found to be influenced by the charge of the entering ligand, the protonation of $[Fe(CN)_5(H_2O)]^{3-}$ itself at one of the cyanide ligands (pK(25 °C, I = 0.10 M) = 2.63 ± 0.12 [32]) and by deprotonation of water in $[Fe(CN)_5(H_2O)]^{3-}$ above pH 13 [11b]. Thus, in this study under specified reaction conditions, the formation rates of the pyridinium-4-aldoxime pentacyanoferrates(II) were only depended on the ionic form of the ligand. The obtained k_f values, presented in Table 4, have been considerably smaller in comparison with values for N-donor cationic ligands [12e] but in agreement with the reported composite formation rates of 15 and 11 M^{-1} s^{-1} for BPA4- and FEPA4-pentacyanoferrates(II) at 22 °C, pH 7.90, I = 0.05 M [4c]. The moderately higher formation rate established for the ambidentate bis-pyridinium-4-aldoxime (TMB4) in comparison with mono-pyridinium-4-aldoximes (PAM4, BPA4 and FEPA4) was in accordance with the presence of two donor groups and the overall higher positive charge of +2. The unexpectedly slow formation, otherwise characteristic for the anionic ligands [11b], could be speculatively associated with the fact that the charge within the protonated pyridinium-4-aldoxime cation is rather dispersed and/or with a conformation effect related to a steric hindrance of E-configurated aldoxime donor group as was suggested for some pyridyl aldoximes [33].

According to a general knowledge, the rate of pyridinium-4-aldoxime substitution in the formed $[Fe(CN)_5(H_nL)]^{(3-n)-}$ complexes, specified as dissociation rate (reverse reaction in Eq. (3)), is strongly dependent on the σ-donor and π-acceptor ability of coordinated ligand [11,12]. Thus a comparative analysis of the kinetics (i.e. lability) of the formed pentacyano(ligand)ferrates(II) was performed by studies of a pyridinium-4-aldoxime substitution from the $[Fe(CN)_5(H_nL)]^{(3-n)-}$ as a function of pH. The rate of dissociation was found to be pH-dependent due to the deprotonation of the bounded aldoxime group. The pH profiles of the dissociation rates are shown in Fig. 4. Consequently, for the examined pyridinium-4-aldoxime pentacyanoferrate(II) complexes with the dissociation reaction scheme involved the following general steps:

$$[Fe(CN)_5(H_nL)]^{(3-n)-} \overset{K_a}{\rightleftarrows} H^+ + [Fe(CN)_5(H_{n-1}L)]^{(4-n)-} \quad (4)$$

$$[Fe(CN)_5(H_nL)]^{(3-n)-} + H_2O \overset{k_{-1}}{\rightarrow} [Fe(CN)_5(H_2O)]^{3-} + H_nL^{n+} \quad (5)$$

$$[Fe(CN)_5(H_{n-1}L)]^{(4-n)-} + H_2O \overset{k_{-2}}{\rightarrow} [Fe(CN)_5(H_2O)]^{3-} + H_{n-1}L^{(n-1)+} \quad (6)$$

where K_a is the ionization constant of the coordinated pyridinium-4-aldoxime. The rate constant is:

$$k_d = \frac{k_{-1} \cdot [H^+] + k_{-2} \cdot K_a}{[H^+] + K_a} \quad (7)$$

Dissociation rate parameters for the release of protonated (k_{-1}) and deprotonated (k_{-2}) pyridinium-4-aldoxime ligand from the $[Fe(CN)_5(H_nL)]^{(3-n)-}$ complex and the ionization constant (K_a) were obtained by the non-linear least-squares fit of the experimental data to Eq. (7) and are presented in Table 5. The apparent formation constants, β_f, for the reaction involving protonated pyridinium-4-aldoximic ligands (Eq. (1)), were deduced from ratio of kinetic parameters, k_f/k_d, (Table 4) and were found to be in reasonable agreement with the values obtained by the mole ratio method. The activation parameters determined for the dissociation reactions confirmed limited S_N1 mechanism for ligand substitution [11].

The magnitude of the dissociation rates suggested that both protonated and deprotonated forms of PAM4, BPA4, FEPA4 and TMB4 are effective σ-donors that bind to the $[Fe(CN)_5]^{3-}$ moiety through the nitrogen atom. Furthermore, the dissociation rate values were consistent with the values deduced for a labile pentacyano(ligand)ferrates(II) containing the exclusively σ-donor or poor π-acceptor ligands [12g–i]. The reduced lability of the examined pentacyano(ligand)ferrates(II) caused by the deprotonation of the coordinated aldoxime group indicated the influence of the charge distribution within the pyridinium-4-aldoxime system on the strength of iron(II)–nitrogen bond. Evidently, increased basicity of aldoximic nitrogen, i.e. σ-donor capability strengthened the iron(II)–nitrogen bond.

According to the literature data the N-coordination of oxime ligand to the metal center (M^{2+}; M = Cu, Pt, Ni, Zn, Fe) often lead to dramatically increased acidity of the oxime group, and was primar-

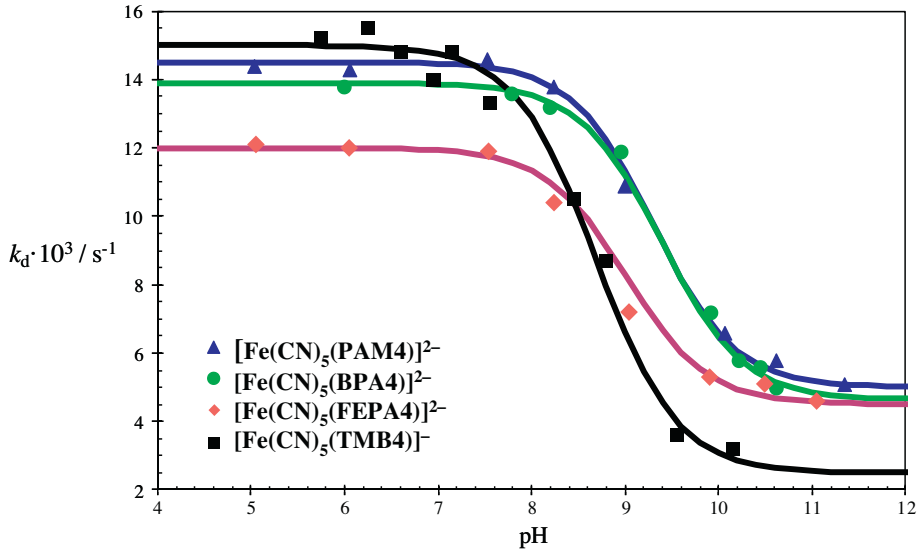

Fig. 4. pH-dependence of the dissociation rate constant for PAM4-, BPA4-, FEPA4- and TMB4-pentacyanoferrate(II) complexes.

Table 5
Rate and activation parameters for the dissociation of pyridinium-4-aldoxime pentacyanoferrate(II) complexes.

[Fe(CN)$_5$(PAM4)]$^{(3-n)-}$		**[Fe(CN)$_5$(BPA4)]$^{(3-n)-}$**		**[Fe(CN)$_5$(FEPA4)]$^{(3-n)-}$**		**[Fe(CN)$_5$(TMB4)]$^{(3-n)-}$**	
Dissociation rate parameters (rate constants in s^{-1}; 25.0 ± 0.5 °C; I = 0.1 M)							
pH ±0.02	$k_d \times 10^3$	pH ±0.03	$k_d \times 10^3$	pH ±0.02	$k_d \times 10^3$	pH ±0.03	$k_d \times 10^3$
5.03	14.4 ± 0.9	5.99	13.8 ± 1.8	5.05	12.1 ± 1.6	5.75	15.2 ± 1.1
6.05	14.3 ± 1.1	7.78	13.6 ± 1.8	6.05	12.0 ± 1.2	6.60	14.8 ± 0.7
7.52	14.6 ± 0.1	8.19	13.2 ± 1.4	7.54	11.9 ± 1.2	7.15	14.8 ± 0.8
8.23	13.8 ± 0.1	8.95	11.9 ± 1.3	8.24	10.4 ± 1.6	7.55	13.3 ± 0.6
8.99	10.9 ± 0.4	9.91	7.2 ± 0.6	9.04	7.2 ± 1.3	8.45	10.5 ± 0.7
10.06	6.6 ± 0.4	10.21	5.8 ± 0.6	9.90	5.3 ± 1.8	8.80	8.7 ± 0.5
10.61	5.8 ± 0.3	10.44	5.6 ± 0.7	10.49	5.1 ± 1.8	9.55	3.6 ± 0.4
11.34	5.1 ± 0.6	10.61	5.0 ± 0.4	11.05	4.6 ± 1.8	10.15	3.2 ± 0.3
$k_{-1} \times 10^3$	$k_{-2} \times 10^3$	$k_{-1} \times 10^3$	$k_{-2} \times 10^3$	$k_{-1} \times 10^3$	$k_{-2} \times 10^3$	$k_{-1} \times 10^3$	$k_{-2} \times 10^3$
14.5 ± 0.7	5.0 ± 0.5	13.9 ± 1.6	4.6 ± 0.6	12.0 ± 1.3	4.5 ± 1.8	15.0 ± 0.9	2.5 ± 0.4
p$K_{a\ coordinated\ PAM4}$		p$K_{a\ coordinated\ BPA4}$		p$K_{a\ coordinated\ FEPA4}$		p$K_{a\ coordinated\ TMB4}$	
9.30 ± 0.5		9.39 ± 0.4		9.01 ± 0.5		8.69 ± 0.6	
Activation parameters ($\Delta H^{\ddagger}$ in kJ mol^{-1}; $\Delta S^{\ddagger}$ in J K^{-1} mol^{-1}; I = 0.1 M)							
pH 6.05 ± 0.02		pH 5.99 ± 0.03		pH 6.05 ± 0.03		pH 6.25 ± 0.03	
t ± 0.1 (°C)	$k_d \times 10^3$	t ± 0.1 (°C)	$k_d \times 10^3$	t ± 0.1 (°C)	$k_d \times 10^3$	t ± 0.1 (°C)	$k_d \times 10^3$
15.9	4.5 ± 0.4	15.3	2.9 ± 0.1	15.2	3.3 ± 0.3	9.8	1.7 ± 0.4
20.2	8.6 ± 0.5	20.1	5.9 ± 0.2	20.3	5.5 ± 0.2	14.8	3.6 ± 0.7
25.0	14.3 ± 1.1	25.0	13.8 ± 1.8	25.0	12.0 ± 1.6	20.5	7.9 ± 0.5
30.3	30.7 ± 1.0	29.7	20.1 ± 0.1	29.8	19.9 ± 0.3	25.0	15.5 ± 1.1
$\Delta H^{\ddagger}$	$\Delta S^{\ddagger}$	$\Delta H^{\ddagger}$	$\Delta S^{\ddagger}$	$\Delta H^{\ddagger}$	$\Delta S^{\ddagger}$	$\Delta H^{\ddagger}$	$\Delta S^{\ddagger}$
88.6 ± 2.3	21.8 ± 0.6	94.3 ± 2.2	34.0 ± 7.2	94.3 ± 3.0	34.5 ± 10.5	95.0 ± 3.0	40.0 ± 15.0

ily assigned to the nature of the M–L bond and to lesser extent to the ligand structure [3]. Interestingly, in contrast to our earlier interpretation that suggested a reduction of the pK_a values of the coordinated aldoxime groups in FEPA4 and BPA4 by more than one pH unit[1] [5b] the significant change in acidity of examined ligands upon coordination has not been observed (Tables 3 and 5). De facto the pK_a value of the coordinated pyridinium-4-aldoximes in the range from 9.0 to 9.5 is undoubtedly supported by the MLCT bands shift toward lower energy upon increasing the pH of the medium over 9. The insignificant change in acidity upon coordination reveals the canceling effect between ligand-to-metal σ-donation and metal-to-ligand π-back donation, and is strongly supported by the established spectroscopic characteristics (FT-IR and NMR) of the pentacyanoferrates(II) complexed with the pyridinium-4-aldoxime type of ligand.

4. Conclusion

The crystalline monohydrate of *N*-methylpyridinium-4-aldoxime chloride (PAM4-Cl) and two polymorphs of anhydrous iodide (PAM4-I) were prepared and characterized. Given that *N*-methylpyridinium-4-aldoxime cation represents a structural foundation of the biologically active mono- and bis-pyridinium-4-aldoximes: chlorides of *N*-benzylpyridinium-4-aldoxime (BPA4-Cl) and

[1] Previously, equilibrium measurements were performed in the reaction mixtures that contained equimolar ligand to [Fe(CN)$_5$(H$_2$O)]$^{3-}$ ratio, which probably resulted in the formation of more than one complex in neutral and slightly alkaline media, leading to the misinterpretation of data.

N-phenacylpyridinium-4-aldoxime (FEPA4-Cl), as well as *N*,*N*′-bis(pyridinium-4-aldoxime)trimethylene dibromide (TMB4-2Br), their chemical properties in aqueous media are compared. The similar ionization abilities of their aldoxime groups in aqueous solution have proven the insignificant effect of the substituent attached to the *N*-methylenepyridinium moiety. Both, the mono- and bis-pyridinium-4-aldoxime ligands react with aquapentacyanoferrate(II) ion by forming mononuclear complexes through the coordination of nitrogen to the iron center, of the either protonated and deprotonated aldoxime group. The produced pyridinium-4-aldoxime pentacyanoferrates(II) are thermodynamically unstable and kinetically labile at 25 °C and $I = 0.1$ M. The pentacyanoferrate(II) moiety does not induce a significant change in acidity of the pyridinium-4-aldoxime ligands upon coordination. This conforms with the results of FT-IR and ^{13}C NMR and UV–Vis spectral analysis which revealed weak π-back bonding capability of the pyridinium-4-aldoxime ligands. Spectroscopic, elemental and thermal analyses of the newly synthesized complex were in optimal accordance with the formula $Na(PAM4)[Fe(CN)_5(PAM4)]\cdot H_2O$.

Acknowledgments

We thank Mrs. S. Matečić-Mušanić (Brodarski Institute, Zagreb, Croatia) for the TGA, DTA and DSC measurements.

This work was supported by the Ministry of Science, Education and Sports of the Republic of Croatia (Grant Nos. 108-1193079-3070 and 119-1193079-1084).

Appendix A. Supplementary data

CCDC 882946, 883098 and 883099 contain the supplementary crystallographic data for this paper. These data can be obtained free of charge via http://www.ccdc.cam.ac.uk/conts/retrieving.html, or from the Cambridge Crystallographic Data Centre, 12 Union Road, Cambridge CB2 1EZ, UK; fax: (+44) 1223-336-033; or e-mail: deposit@ccdc.cam.ac.uk. Supplementary data associated with this article can be found, in the online version, at http://dx.doi.org/10.1016/j.poly.2012.07.077.

References

[1] F. Mancin, P. Tecilla, U. Tonellato, Eur. J. Org. Chem. (2000) 1045.
[2] (a) F. Mancin, P. Tecilla, U. Tonellato, Langmuir 16 (2000) 227;
(b) A.K. Yatsimirsky, P. Gomez-Tagle, S. Escalante-Tovar, L. Ruiz-Ramirez, Inorg. Chim. Acta 273 (1998) 167;
(c) R. Breslow, D. Chipman, J. Am. Chem. Soc. 87 (1965) 4195.
[3] C.J. Milios, T.C. Stamatatos, S. Perlepes, Polyhedron 25 (2006) 134.
[4] (a) Z. Koričanac, K. Kariljković-Rajić, B. Stanković, Talanta 37 (1990) 535;
(b) N. Burger, V. Hankonyi, Anal. Lett. 25 (1992) 1355;
(c) N. Burger, V. Hankonyi, Z. Smerić, Z. Phys. Chem. (Leipzig) 271 (1990) 787;
(d) N. Burger, V. Hankonyi, Polyhedron 5 (1986) 663;
(e) N. Burger, Z. Smerić, V. Hankonyi, Acta Pharm. Jugosl. 36 (1986) 15;
(f) N. Burger, V. Karas-Gašparec, Talanta 31 (1984) 169;
(g) N. Burger, V. Karas-Gašparec, Talanta 28 (1981) 323;
(h) V. Hankonyi, V. Ondrušek, V. Karas-Gašparec, Z. Binenfeld, Z. Phys. Chem. (Leipzig) 251 (1972) 280.
[5] (a) B. Foretić, I. Picek, V. Damjanović, D. Cvijanović, D. Milić, J. Mol. Struct. 1019 (2012) 196;
(b) B. Foretić, I. Picek, I. Đilović, N. Burger, Inorg. Chim. Acta 363 (2010) 1425.
[6] M. Jokanović, M. Prostran, Curr. Med. Chem. 16 (2009) 2177.
[7] (a) E. Abele, R. Abele, E. Lukevics, Chem. Heterocycl. Compd. 39 (2003) 847;
(b) S.K. Bognar, B. Foretić, Ž. Vukelić, T. Gulin, D. Ježek, Croat. Chem. Acta 81 (2008) 67.
[8] See for example: E. Ilkowska, K. Lewiński, R. Van Eldik, G. Stochel, J. Biol. Inorg. Chem. 4 (1999) 302.
[9] See for example: H. Winnischofer, F.M. Engelmann, H.E. Toma, K. Araki, H.R. Rechenberg, Inorg. Chim. Acta 338 (2002) 27.
[10] (a) B.J. Coe, S.P. Foxon, E.C. Harper, J. Raftery, R. Shaw, C.A. Swanson, I. Asselberghs, K. Clays, B.S. Brunschwig, A.G. Fitch, Inorg. Chem. 48 (2009) 1370;
(b) B.J. Coe, J.L. Harries, L.A. Jones, I. Asselberghs, K. Clays, B.S. Brunschwig, J.A. Harris, J. Garin, J. Orduna, J. Chem. Soc. 128 (2006) 12192.
[11] (a) D.H. Macartney, Rev. Inorg. Chem. 9 (1988) 101;
(b) H.E. Toma, A.A. Batsta, H.B. Gray, J. Am. Chem. Soc. 104 (1982) 7509.
[12] (a) J.B. Luiz, G.J. Leigh, F.S. Nunes, Polyhedron 21 (2002) 2137;
(b) Y. Baran, A. Ulgen, Int. J. Chem. Kinet. 30 (1998) 415;
(c) C. Chen, M. Wu, A. Yeh, T.Y.R. Tsai, Inorg. Chim. Acta 267 (1998) 81;
(d) S.da S.S. Borges, A.L. Coelho, I.S. Moreira, Polyhedron 13 (1994) 1015;
(e) D.H. Macartney, L.J. Warrack, Can. J. Chem. 67 (1989) 1774;
(f) D.H. Macartney, A. McAuley, Inorg. Chem. 20 (1981) 748;
(g) D.H. Macartney, A. McAuley, J. Chem. Soc., Dalton Trans. (1981) 1780;
(h) H.E. Toma, J.M. Martins, E. Giesbrecht, J. Chem. Soc., Dalton Trans. (1978) 1610;
(i) H.E. Toma, J.M. Malin, Inorg. Chem. 13 (1974) 1772;
(j) H.E. Toma, J.M. Malin, E. Giesbrecht, Inorg. Chem. 12 (1973) 2084;
(k) H.E. Toma, J.M. Malin, Inorg. Chem. 12 (1973) 2080;
(l) H.E. Toma, J.M. Malin, Inorg. Chem. 12 (1973) 1039.
[13] I. Hagedorn, I. Stark, K. Schoene, H. Schenkel, Arzneim.-Forsch./Drug Res. 28 (1978) 2055.
[14] L. Leitis, E. Liepinis, D. Jansone, M.V. Shimanskaya, Latv. PSR Zinat. Akad. Vestis. Kim. Ser. 6 (1984) 719.
[15] J.J. Kaminski, K.W. Knutson, N. Bodor, Tetrahedron 34 (1978) 2857.
[16] Oxford Diffraction, CrysAlis CCD and CrysAlis RED, Versions 171.32.24, 2008.
[17] G.M. Sheldrick, Acta Crystallogr., Sect. A 64 (2008) 112.
[18] A.L. Spek, J. Appl. Crystallogr. 36 (2003) 7.
[19] M. Nardelli, J. Appl. Crystallogr. 28 (1995) 659.
[20] (a) L.J. Farrugia, J. Appl. Crystallogr. 30 (1997) 565;
(b) C.F. Macrae, P.R. Edgington, P. McCabe, E. Pidcock, G.P. Shields, R. Taylor, M. Towler, J. van de Streek, J. Appl. Crystallogr. 39 (2006) 453.
[21] M. Boccio, A. Sayago, G. Asuero, Int. J. Pharm. 318 (2006) 70.
[22] F.H. Allen, O. Kennard, D.G. Watson, L. Brammer, A.G. Orpen, J. Chem. Soc., Perkin Trans. II (1987) S1.
[23] (a) R. Odžak, I. Halasz, S. Tomić, D. Matković-Čalogović, Acta Crystallogr., Sect. E 62 (2006) o2423;
(b) M. Jukić, A. Hergold-Brundić, M. Cetina, A. Nagl, J. Vorkapić-Furač, Struct. Chem. 14 (2003) 597;
(c) C.D. Bustamante, R.J. Staples, Z. Kristallogr. NCS 214 (1999) 141;
(d) W. Van Havere, A.T.H. Lenstra, H.J. Geise, G.R. Van Den Berg, H.P. Benschop, Acta Crystallogr., Sect. B 38 (1982) 1635;
(e) W. Van Havere, A.T.H. Lenstra, H.J. Geise, G.R. Van Den Berg, H.P. Benschop, Acta Crystallogr., Sect. B 38 (1982) 2516.
[24] B. Foretić, N. Burger, Monatsh. Chem. 135 (2004) 261.
[25] (a) J. Gi Jee, O.C. Kwun, Bull. Korean Chem. Soc. 5 (1984) 44;
(b) R.A. Lalancette, W. Furey, J.N. Costanzo, P.R. Hemmes, F. Jordan, Acta Crystallogr., Sect. B 34 (1978) 2950;
(c) P. Hemmes, J.N. Costanzo, F. Jordan, J. Phys. Chem. 82 (1978) 387.
[26] K. Schoene, E.M. Strake, Biochem. Pharmacol. 20 (1971) 1041.
[27] (a) V. Mohaček Grošev, B. Foretić, O. Gamulin, Spectrochim. Acta A 78 (2011) 1376;
(b) T. Stepanenko, L. Lapinski, M.J. Novak, L. Adamowicz, Vib. Spectrosc. 26 (2001) 65.
[28] R. Middleton, J.R. Thornback, G. Wilkinson, J. Chem. Soc., Dalton Trans. (1980) 174.
[29] K. Nakamoto, Infrared and Raman Spectra of Inorganic and Coordination Compounds, fifth ed., John Wiley and Sons, New York, 1997. p. 266.
[30] P.J. Morando, V.I.E. Bruyere, Miguel A. Blesa, Transition Met. Chem. 8 (1983) 99.
[31] (a) R.B. Lanjewar, M.R. Lanjewar, Int. J. Knowl. Eng. 3 (2012) 61;
(b) D.B. Soria, P.J. Aymonino, Spectrochim. Acta A 55 (1999) 1243;
(c) R.B. Lanjewar, S. Kawata, S. Kitagawa, M. Katada, J. Therm. Anal. 50 (1997) 375;
(d) R.B. Lanjewar, S. Kawata, T. Nawa, S. Kitagawa, A.N. Garg, M. Katada, Thermochim. Acta 287 (1996) 111;
(e) E.E. Sileo, M.G. Garcia, A. Posse, P.J. Morando, M.A. Blesa, Polyhedron 6 (1987) 1757;
(f) M.M. Chamberlain, A.F. Greene Jr., J. Inorg. Nucl. Chem. 25 (1963) 1471.
[32] J.M. Malin, R.C. Koch, Inorg. Chem. 17 (1978) 752.
[33] N.Y. Murakami Iha, H.E. Toma, Inorg. Chim. Acta 81 (1984) 181.